

A NEW METHOD TO CONSTRAIN THE ORIGINS OF DARK MATTER-FREE GALAXIES AND THEIR UNUSUAL GLOBULAR CLUSTERS

NATHAN W. C. LEIGH^{1,2}, GIACOMO FRAGIONE^{3,4,5}

¹Departamento de Astronomía, Facultad de Ciencias Físicas y Matemáticas, Universidad de Concepción, Concepción, Chile

²Department of Astrophysics, American Museum of Natural History, Central Park West and 79th Street, New York, NY 10024

³Racah Institute for Physics, The Hebrew University, Jerusalem 91904, Israel

⁴Center for Interdisciplinary Exploration & Research in Astrophysics (CIERA), Evanston, IL 60202, USA and

⁵Astronomy Department, Harvard University, 60 Garden St., Cambridge, MA 02138, USA

Draft version December 15, 2024

ABSTRACT

We present a novel method to uniquely constrain the collisional evolution of globular cluster (GC) populations that are hypothesized to have recently undergone an episode of violent relaxation due to a strong galaxy-galaxy interaction. We show via analytic methods that numerical simulations combined with observed constraints on the GC luminosity function can be used to constrain the GC mass function immediately after the assumed episode of violent relaxation. In order to apply our method, we first explore the observational evidence for a collisional origin for the recently discovered dark matter (DM)-free ultra-diffuse galaxies observed in the NGC 1052 group. We compute the timescales for infall to the central nucleus due to dynamical friction (DF) for the GCs in NGC 1052-DF2 and NGC 1052-DF4, using the shortest of these times to constrain how long ago such an interaction could have occurred. We find that two out of ten GCs in NGC 1052-DF2 and one out of seven in NGC 1052-DF4 have DF timescales less than a Hubble time. We go on to quantify the initial GC numbers and densities needed for significant collisional evolution to occur within the allotted times. Finally, we apply our method to these galaxies, in order to illustrate its efficacy in constraining their dynamical evolution post-violent relaxation. Our results motivate more complete observations of the GC luminosity functions in these galaxies, which can be used to constrain the origins of the hypothesized DM-free galaxies, by combining the method presented here with a suite of numerical simulations.

Keywords: galaxies: galaxy clusters – galaxies: interacting galaxies – Globular star clusters – Stellar dynamics

1. INTRODUCTION

Recently, [Van Dokkum et al. \(2018a\)](#) reported the discovery of a dark matter (DM)-free galaxy, namely the ultra-diffuse galaxy NGC 1052-DF2. This galaxy is one of 23 objects identified in the group NGC 1052 using the Dragonfly Telescope Array ([Abraham & van Dokkum 2014](#); [Behroozi, Wechsler & Conroy 2013](#)), and subsequently followed up using the ACS on the Hubble Space Telescope (HST) ([Cohen et al. 2018](#)). The authors used the radial velocities of ten globular clusters (GCs) orbiting within the potential of this galaxy to constrain its velocity dispersion to be $\sim 10 \text{ km s}^{-1}$ ([Van Dokkum et al. 2018b](#)). They report a total luminous mass of $2 \times 10^8 M_{\odot}$ and, from its velocity dispersion, a total mass (seen and unseen) of $3.4 \times 10^8 M_{\odot}$. This implies a ratio for $M_{\text{halo}}/M_{\text{stars}}$ of order unity, where M_{stars} is the total stellar mass and M_{halo} is the total galaxy mass including the DM halo. Thus, the observations are consistent with there being no DM in this galaxy, since this ratio is typically at least a factor of ~ 400 higher ([Behroozi, Wechsler & Conroy 2013](#)). The authors infer from this that DM is not always coupled to baryonic matter on galactic scales.

In a subsequent paper, a second DM-free galaxy was reported. NGC 1052-DF4 is a low surface brightness galaxy in the same group, identified by [Van Dokkum et al. \(2019\)](#). The authors infer a total enclosed mass within 7 kpc of $0.4^{+1.2}_{-0.3} \times 10^8 M_{\odot}$, and a total stellar mass of $(1.5 \pm 0.4) \times 10^8 M_{\odot}$ within the same enclosed radius. They conclude that this galaxy is consistent with having no DM. As with NGC 1052-DF2, this galaxy hosts an unusually bright population of GCs, but more extended than NGC 1052-DF2.

The existence of such dark-matter deficient galaxies is still

disputed, however. For example, [Trujillo et al. \(2019\)](#) recently argued that the distance to NGC 1052 is only 13 Mpc instead of the 20 Mpc measured by [Van Dokkum et al. \(2018a\)](#). The authors further argue that this can explain *both* the proposed lack of DM and the anomalous GC populations. With that said, [Van Dokkum et al. \(2018c\)](#) subsequently showed that the colour-magnitude diagram is strongly influenced by blends, causing the appearance of a false red giant branch tip about roughly twice as bright as the true red giant branch tip. This translates into an underestimate of the true distance by a factor of ~ 1.4 . [Laporte, Agnello & Navarro \(2019\)](#) further argue that an underestimate of the uncertainty on the mass of the host galaxy could also explain the need to invoke DM-free halos in these host galaxies. As an independent explanation for the apparently curious observational results of [Van Dokkum et al. \(2018a\)](#), [Kroupa et al. \(2019\)](#) proposed that the apparent lack of DM in these galaxies can be understood within the context of MODified Newtonian Dynamics (MOND), which should cause a weaker self-gravity in the outskirts of galaxies when in close proximity to a massive host. In spite of these interesting counter-arguments to the work of [Van Dokkum et al. \(2018a\)](#), these works do not explain the curious GC luminosity function and spatial distribution, at least not without a paucity of low-mass GCs relative to the Milky Way and other galaxies (see Figure 1 below).

How might a DM-free galaxy form? One possibility relies on impulsive heating mediated by tidal forces. This can in principle alter a rotationally-supported disk of stars and gas into a spheroidal structure. Often termed tidal stripping or shocking (e.g. [Gnedin, Hernquist & Ostriker 1999](#); [Mayer et al. 2007](#)), this mechanism may require an additional pro-

cess to fully deplete the new spheroid of its gas (e.g. [Mac Low & Ferrara 1999](#)). [D’Onghia et al. \(2009\)](#) considered direct interactions between dwarf disk galaxies and more massive interlopers. Using numerical simulations, the authors describe a mechanism they term “resonant stripping” that can strip dwarf disk galaxies of their stars. The mechanism occurs for prograde encounters with large mass ratios of order ~ 10 – 100 . Resonant stripping happens when the spin and orbital frequencies are comparable. This pulls the gas and stars out of the galaxy, since they comprise the disk, whereas the DM is not affected since it is pressure-supported and has no spin frequency.

Several authors have pointed out that the observed populations of GCs in NGC 1052-DF2 and NGC 1052-DF4 are both peculiar ([Emsellem et al. 2019](#); [Fensch et al. 2019](#)). In particular, where are all the low-mass GCs? And why are the observed GCs so centrally concentrated? These galaxies lie well off the previously reported relation between the total GC mass in galaxies and the total mass of their DM halos ([Choksi & Gnedin 2018](#)). Figure 1 shows a comparison between these two GC populations and the Milky Way (MW) GC population. First, even though the MW is much more massive and also more extended than either NGC1052-DF2 or NGC1054-DF4, we see that the latter galaxies have a larger fraction of very bright/massive GCs at small Galactocentric radii when compared to the MW’s GCs. As shown by the open squares and dotted histograms, this remains the case, although to a lesser extent, if one adopts the distance estimate provided in [Trujillo et al. \(2019\)](#). Second, the nearest giant elliptical galaxy to the MW, namely NGC 5128 (i.e., Centaurus A), is home to a population of GCs whose mass function is similar to that of the M31 GC system but with a larger mean GC mass (and also mean mass-to-light ratio), and indistinguishable from the MW’s GC system (due mostly to the much smaller sample size in the MW compared to NGC 5128) (e.g. [Taylor et al. 2015](#)). The GC populations in NGC 1052-DF2 and NGC 1052-DF4 are therefore probable outliers in previously reported studies looking at, for example, GC mass functions and GC specific frequencies in different types of galaxies (e.g. [Harris, Gretchen & Alessi 2013](#); [Harris 2016](#)). Additionally, the GCs in NGC1052-DF2 and NGC1052-DF4 are significantly more concentrated at small (projected) galactocentric distances compared to the brightest GCs in the sample from [Harris \(1996, 2010 update\)](#).

In this paper, we consider a scenario in which the ultra-diffuse galaxies NGC 1052-DF4 and NGC 1052-DF2, posited in the literature to be DM-free, were dynamically stripped of their DM haloes. This could have occurred, for example, due to a strong interaction with a more massive nearby galaxy (e.g. [D’Onghia et al. 2009](#)) or even a direct galaxy-galaxy collision (e.g. [Silk 2019](#)), which triggered an episode of violent relaxation in their GC populations ([Lynden-Bell 1967](#)). We then consider the subsequent dynamical evolution of such a disturbed GC population. First, we compute numerically the mass, density and velocity dispersion profiles of both NGC 1052-DF2 and NGC 1052-DF4. These are used to compute the radial profiles of the DF timescales in both galaxies for a typical GC with a mass of $10^6 M_\odot$. Second, we calculate the dynamical friction timescales for all GCs reported in [Van Dokkum et al. \(2018b\)](#) and [Van Dokkum et al. \(2019\)](#), and compare them to a Hubble time. If a computed DF timescale is much shorter than a Hubble time, we interpret this as evidence that they did not form in their currently observed positions, motivating consideration of other formation scenarios.

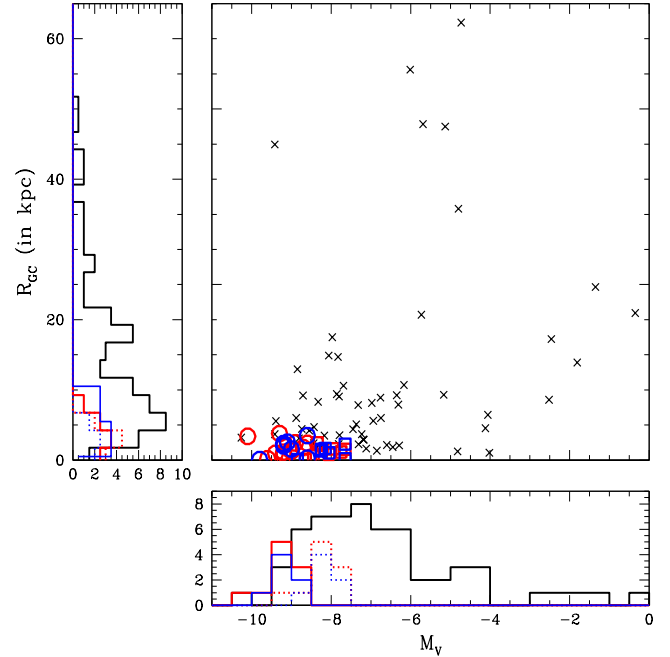


Figure 1. The integrated V-band magnitudes for the Milky Way GC population (shown by the black crosses) are plotted against their Galactocentric distances, using all available data in [Harris \(1996, 2010 update\)](#). For comparison, we also plot the same observed quantities for the GCs in NGC1052-DF2 (red open circles) and NGC1052-DF4 (blue open circles) using the distance of 20 Mpc assumed in [Van Dokkum et al. \(2018a\)](#). The open red and blue squares, as well as the dotted histograms, show the same thing but adopting the distance estimate of 13 Mpc found by [Trujillo et al. \(2019\)](#). Note that we have not included the new GC candidates reported in [Trujillo et al. \(2019\)](#), since this comparison has already been done in their Figures 11 and 12.

We further present a novel method to constrain the collisional evolution for such GC populations post-galaxy-galaxy interaction. We show via analytic methods that numerical simulations combined with observed constraints on the GC luminosity function can be used to constrain the GC mass function immediately post-interaction. Our methods and results are presented in Section 2. In Section 3, we discuss the implications of our results for understanding the origins of the hypothesized DM-free galaxies and their GC populations, and make predictions for the observed properties of future discoveries in this potentially new class of galaxies. Finally, we conclude in Section 4.

2. CALCULATIONS

In this section, we compute numerically the mass, density and velocity dispersion profiles of both NGC 1052-DF2 and NGC 1052-DF4. These are used to compute order-of-magnitude estimates for the radial profiles of the DF timescales in both galaxies for a typical GC with a mass of $10^6 M_\odot$. We also calculate the dynamical friction timescales for all GCs reported in [Van Dokkum et al. \(2018b\)](#) and [Van Dokkum et al. \(2019\)](#) and compare these to a Hubble time.

2.1. Mass, density and velocity dispersion profiles

In order to calculate the density and velocity dispersion profiles, we must first calculate the mass enclosed within radius r . This requires obtaining the free parameters in the fitting functions from previous observational studies focused on the two galaxies in our sample. [Cohen et al. \(2018\)](#) fit the sur-

face brightness profile of the dwarf spheroidal galaxy NGC 1052-DF4 using a Sersic model. We follow these authors and adopt a Sersic index of $n = 0.79$, a central surface brightness of $\mu(V_{606,0}) = 23.7$ and a major axis half-light radius of $R_e = 1.6$ kpc, and assume a distance to the galaxy of $D = 20$ Mpc.

We perform an analogous calculation for NFC 1052-DF2. [Cohen et al. \(2018\)](#) also fit the surface brightness profile of the dwarf spheroidal galaxy NGC 1052-DF2 using a Sersic model. We adopt the same parameters as these authors, specifically a Sersic index of $n = 0.55$, a central surface brightness of $\mu(V_{606,0}) = 24.2$, a (major-axis) half-light radius of $R_e = 1.8$ kpc, and a distance to the galaxy of $D = 20$ Mpc.

To calculate the mass profiles for both galaxies, we adopt Equation A2 for the enclosed mass $M(r)$ from [Terzic & Graham \(2005\)](#):

$$M_{\text{gal}}(r) = 4\pi\rho_0 R_e^3 n b^{n(p-3)} \gamma(n(3-p), z), \quad (1)$$

where γ is the incomplete gamma function, and the dimensionless variable is defined as:

$$z = b \left(\frac{r}{R_e} \right)^{1/n}, \quad (2)$$

and, after a little math:

$$\rho_0 = \frac{\sqrt{\pi}}{4R_e} \Upsilon_0 I_e b^{n(1-p)}. \quad (3)$$

Finally, the mass-to-light ratio for an old stellar population is typically $\Upsilon_0 = M/L \sim 2 M_\odot/L_\odot$, and the variable p can be approximated by the relation:

$$p = 1 - \frac{0.6097}{n} + \frac{0.055}{n^2}. \quad (4)$$

We adopt $n = 0.79$, for which Equation 4 reduces to $p = 0.3163$. Finally, the radial velocity dispersion profile is computed using Equation A5 in [Terzic & Graham \(2005\)](#).

2.2. Dynamical friction timescales

The term dynamical friction, in its original form, refers to the gravitational focusing of particles into a wake by a massive perturber as it travels through a homogeneous background medium of constant density ([Chandrasekhar 1943](#)). As applied to GCs orbiting in the potentials of their host galaxy ([Tremaine, Ostriker & Spitzer 1975](#)), this generates a damping force due to the gravitational tug of the trailing wake, and ultimately removes energy and angular momentum from the GC's orbit, causing it to (eventually) spiral into the host galaxy's centre of mass. The timescale for dynamical friction to operate is approximately given by ([Binney & Tremaine 1987](#); [Gnedin, Ostriker & Tremaine 2014](#)):

$$\tau_{\text{df}} = \frac{1.17 M_{\text{gal}}(r)r}{\ln \Lambda m_{\text{GC}} \sigma(r)}, \quad (5)$$

where $M_{\text{gal}}(r)$ and $\sigma(r)$ are, respectively, the enclosed galaxy mass and the stellar velocity dispersion at a distance r from the centre of mass of the galaxy, m_{GC} is the mass of the orbiting GC and $\ln \Lambda$ is the Coulomb logarithm for which we adopt $\ln \Lambda = 10$ (for details see [Arca-Sedda & Capuzzo-Dolcetta 2017](#); [Nusser 2018](#)).

2.3. Radial profiles

The radial dependences of the host galaxy enclosed masses, densities and velocity dispersions are shown in Figure 2. We also show the DF timescales as a function of distance from the centre of mass of the host galaxy using Equation 5, for a hypothetical GC with total mass $m_{\text{GC}} = 10^6 M_\odot$. The dashed lines in the top panel show the corrected DF timescales assuming

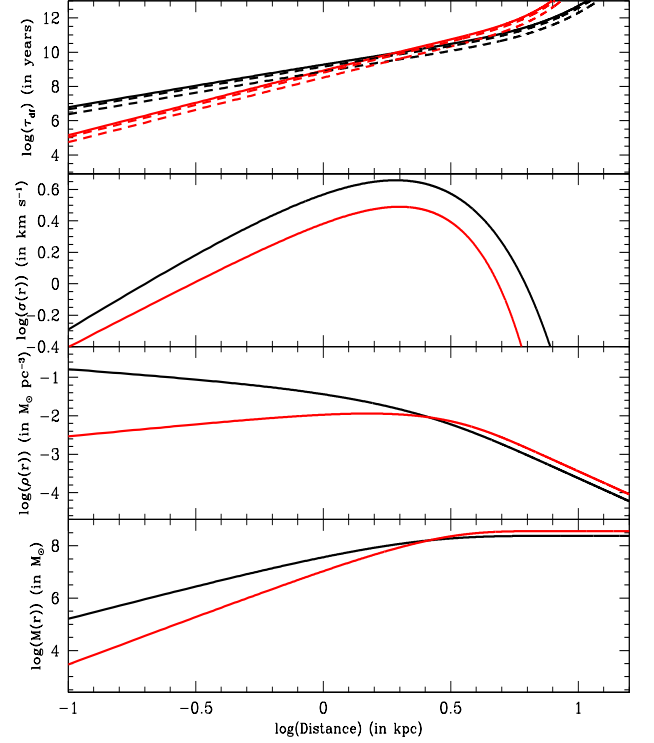


Figure 2. From bottom to top, each panel shows the radial dependence of, respectively, the enclosed mass $M_{\text{gal}}(r)$, the mass density $\rho(r)$, the stellar velocity dispersion $\sigma(r)$ and the DF timescale τ_{df} for a hypothetical GC with total mass $m_{\text{GC}} = 10^6 M_\odot$ and assuming for the Coulomb logarithm $\ln \Lambda = 6$, for the galaxies NGC 1052-DF4 (black) and NGC 1052-DF2 (red). The dashed lines in the top panel show how the DF timescales are expected to change assuming eccentric orbits, adopting the minimum and maximum correction factors provided in [Gnedin, Ostriker & Tremaine \(2014\)](#) (see text for more details).

eccentric orbits. Specifically, we multiply the DF timescales by the minimum and maximum correction factors provided in [Gnedin, Ostriker & Tremaine \(2014\)](#), which are 0.4 and 0.8, respectively (see Section 2.4). *More eccentric orbits reduce the DF timescale at a given galactocentric distance.*

The velocity dispersion peaks very close to the observed projected galactocentric distances of many GCs in both NGC 1052-DF2 and NGC 1052-DF4, and declines rapidly on either side of this peak. We caution, however, that the peaks of our velocity distributions, in particular for NGC 1052-DF2, are slightly lower than that reported in [Van Dokkum et al. \(2018b\)](#). This could translate into mildly higher DF timescales for this galaxy than expected from the velocity measurements of [Van Dokkum et al. \(2018b\)](#). This should be accounted for when trying to infer the *true* DF timescales. However, these analytic estimates are at best approximations (see the next section). In spite of this, our basic conclusions are consistent with those of [Dutta Chowdhury, van den Bosch & van Dokkum \(2019\)](#) and [Nusser \(2018\)](#).

2.4. Dynamical friction timescales for individual GCs

In this section, we compute DF timescales for all seven and ten GCs orbiting within, respectively, the galaxies NGC 1052-DF4 and NGC 1052-DF2 reported in [Van Dokkum et al. \(2019\)](#) and [Van Dokkum et al. \(2018b\)](#).

Using Equations 5 and Equation A5 from [Terzic & Graham \(2005\)](#), we show the computed DF timescales in Figure 3, as-

Table 1

The computed properties for all globular clusters in both NGC 1052-DF2 (top 10 rows) and NGC 1052-DF4 (bottom 7 rows).

GC ID	Mass (M_\odot)	Distance (kpc)	τ_{df} (yr)
39	6.7×10^5	7.55	9.7×10^{12}
59	4.7×10^5	4.91	7.3×10^{11}
71	5.1×10^5	2.57	5.2×10^{10}
73	1.4×10^6	6.77	1.8×10^{12}
77	8.9×10^5	7.55	7.4×10^{12}
85	6.2×10^5	2.26	2.7×10^{10}
91	6.2×10^5	1.55	7.1×10^9
92	7.4×10^5	1.94	1.2×10^{10}
98	3.9×10^5	3.59	2.4×10^{11}
101	3.5×10^5	4.77	8.3×10^{11}
2726	6.2×10^5	4.69	1.6×10^{11}
2537	6.2×10^5	4.08	1.0×10^{11}
2239	3.5×10^5	0.57	1.4×10^9
1968	1.1×10^6	2.90	2.3×10^{10}
1790	5.1×10^5	3.17	6.1×10^{10}
1452	5.6×10^5	5.13	2.3×10^{11}
943	3.5×10^5	7.01	1.4×10^{12}

Table 2

Fraction of clusters (out of the total) with $\tau_{df} < 10^{10}$ yr for different assumptions for GC eccentricity and projected distance (see Section 2.4).

Galaxy	Eccentricity	Distance	Fraction
NGC 1052-DF2	circular	r_{obs}	10%
NGC 1052-DF2	$(J/J_c(E))^{0.4}$	r_{obs}	10%
NGC 1052-DF2	$(J/J_c(E))^{0.8}$	r_{obs}	10%
NGC 1052-DF2	circular	$r_{obs}/\cos\theta$	5.6%
NGC 1052-DF4	circular	r_{obs}	29%
NGC 1052-DF4	$(J/J_c(E))^{0.4}$	r_{obs}	29%
NGC 1052-DF4	$(J/J_c(E))^{0.8}$	r_{obs}	29%
NGC 1052-DF4	circular	$r_{obs}/\cos\theta$	13%

suming a distance to NGC 1052-DF4 and NGC 1052-DF2 of 20 Mpc. The left panel shows the DF timescales as a function of the total GC mass, assuming a mass-to-light ratio of $2 M_\odot/L_\odot$, whereas the right panel shows the same timescales but as a function of the projected galactocentric distance. The horizontal solid line demarcates a Hubble time. One GC has a DF timescale shorter than a Hubble time in NGC 1052-DF4 (black open circles), whereas two out of ten GCs have DF timescales less than a Hubble Time in NGC 1052-DF2 (red open circles).

If the computed DF timescales in Table 2 are taken at face value, this suggests that even if these GCs began further out in their host galaxy potentials and migrated in to their currently observed galactocentric distances, we have been fortuitous to have caught *both* GC 2239 in NGC 1052-DF4 and GC 91 in NGC 1052-DF2 just before inspiral in to the nucleus.

We caution that our computed DF timescales should come along with significant uncertainty, stemming mostly from the GCs' true or 3D distances from their host galaxy centre of mass, which are not known and could be larger than their observed *projected* galactocentric distances (although, as discussed in Nusser (2018), this simple analytic calculation also suffers from issues related to, for example, a more complicated galaxy mass profile than is represented by our analytic approximations, interactions between GCs, etc.).

Is it possible that the eccentricities of the observed GCs are non-negligible? If so, this could yield DF timescales shorter than we find by assuming that they are on circular orbits. To

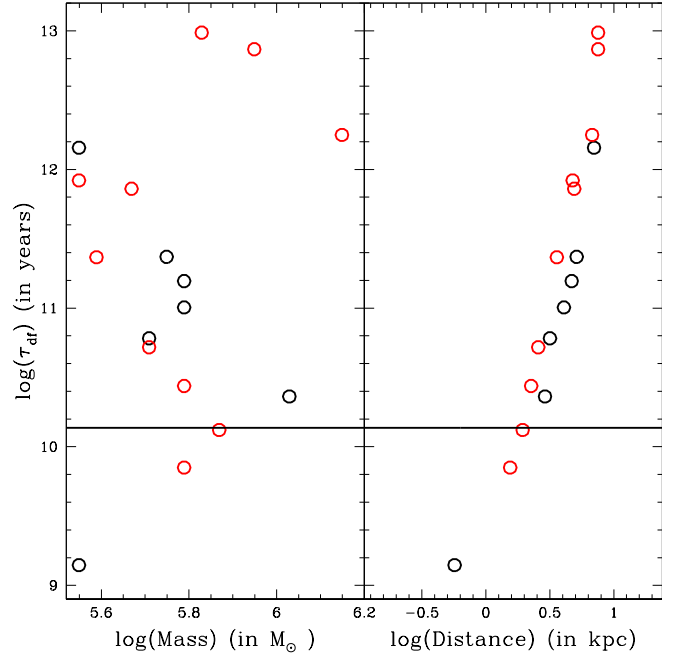


Figure 3. The DF timescales are shown as a function of the total GC mass (left panel) assuming a mass-to-light ratio of $2 M_\odot/L_\odot$ for all GCs, and as a function of the projected galactocentric distance (right panel) in kpc. These results are shown for all 7 GCs in NGC 1052-DF4 (black), and all 10 GCs in NGC 1052-DF2 (red). The horizontal solid line demarcates a Hubble time.

include the effect of the eccentricity, we consider a reduced DF timescale:

$$\tau_{df,ecc} = \tau_{df} \left(\frac{J}{J_c(E)} \right)^\alpha, \quad (6)$$

where $J/J_c(E)$ is the ratio of the orbital angular momentum to its maximum value for a given energy E . The values of the exponent given in the literature range from $\alpha \approx 0.4$ (Colpi et al. 1999) to $\alpha \approx 0.8$ (Lacey & Cole 1993).

To quantify this effect, we use a Monte Carlo approach. In our calculation, we assume that the ratio $J/J_c(E)$ is uniformly distributed for the GC population under consideration. We sample $J/J_c(E)$ for 10^4 realizations and compute the typical DF timescale in Eq. 6. We find that the number of GCs expected to have $\tau_{df,ecc} < 10^{10}$ yr remains constant both for NGC 1052-DF2 and NGC 1052-DF4. Thus, the (unknown) eccentricities of the observed GCs do not significantly affect their DF timescales.

Next, we attempt to quantify the possible importance of projection effects. Specifically, could any of the GCs (especially the three with $\tau_{df} < \tau_{Hubble}$ in Figure 3) have true 3D galactocentric distances much larger than their observed *projected* distances? If so, this is important, since it would give rise to an artificially short DF timescale for some GCs. To address this possibility, we assume that the true distance r_{true} from the centre of mass of the host galaxy is related to the observed distance r_{obs} (see Tab. 2) by:

$$r_{obs} = r_{true} \cos\theta, \quad (7)$$

where θ is the angle between the true vector and the projected vector. We then sample $\cos\theta$ uniformly for 10^4 realizations, compute r_{true} and τ_{df} via Eq. 5. In the case of NGC 1052-DF2, we find that the probability for GC 77 to still have τ_{df} less than a Hubble time is $\sim 56\%$. In the case of NGC 1052-DF4, the

probability to have two or one GCs with τ_{df} less than a Hubble time is $\sim 43\%$ and $\sim 47\%$, respectively.

Thus, neither non-zero eccentricities for the observed GCs or projection affects should significantly affect any of our conclusions thus far.

Finally, what if the distances to NGC 1052-DF2 and NGC 1052-DF4 are wrong, as suggested in [Trujillo et al. \(2019\)](#)? These authors argue for a distance of only 13 Mpc instead of the 20 Mpc adopted in [Van Dokkum et al. \(2018a\)](#). We have computed the dynamical friction timescales under the assumption that both NGC 1052-DF2 and NGC 1052-DF4 are DM-free. However, assuming a distance of only 13 Mpc, [Trujillo et al. \(2019\)](#) argued that the minimum DM mass would be $\sim 10^9 M_\odot$, with a stellar mass of $\sim 10^7 M_\odot$, for NGC 1052-DF2. If we account for this in Eq. 5, along with the different GC V-band magnitudes and galactocentric distances (see Fig. 1), τ_{df} would be a factor of ~ 4 longer than if these galaxies are DM-free. Thus, only the GC 2239 in NGC 1052-DF4 would have a DF timescale shorter than a Hubble time.

Independent of the issue of dynamical friction, it is remarkable that the GC system mass is a few percent of the galaxy stellar mass in both galaxies, whatever distance is assumed. These galaxies remain peculiar in the well-known cosmological scaling relations, compared to, for example, dwarf galaxies which have similar stellar masses (see e.g. [Gnedin, Ostriker & Tremaine 2014](#); [Forbes et al. 2018](#)). Thus, some mechanism must have resulted in NGC 1052-DF2 and NGC 1052-DF4 having a large fraction of their baryonic mass in the form of massive luminous GCs.

2.5. The rate of direct GC-GC collisions

Could the presently observed GC populations have been modified (post-violent relaxation due to the hypothesized recent galaxy-galaxy interaction) via direct collisions and/or mergers? As suggested by [Dutta Chowdhury, van den Bosch & van Dokkum \(2019\)](#), GC-GC interactions could help to impede dynamical friction, continually stirring the centrally concentrated GC population and preventing them from falling in to the very centre of their host galaxy. Both [Nusser \(2018\)](#) and [Dutta Chowdhury, van den Bosch & van Dokkum \(2019\)](#) find in their N-body simulations that such strong GC-GC interactions do occur frequently and that this could indeed contribute to slowing the rate of DF. In this section we ask: What about direct GC-GC collisions?

To address this question, we first compute the mean times corresponding to direct collisions between GCs.

$$\tau_{\text{coll}} = 1.1 \times 10^{10} \left(\frac{1 \text{ pc}}{R_{\text{GC,max}}} \right)^3 \left(\frac{10^3}{n_{\text{GC}}} \right)^2 \times \left(\frac{v_{\text{rms}}}{5 \text{ km s}^{-1}} \right) \left(\frac{0.5 M_\odot}{\bar{m}_{\text{GC}}} \right) \left(\frac{0.5 R_\odot}{\bar{r}_{\text{GC}}} \right) \text{ yr}, \quad (8)$$

where \bar{r}_{GC} is the mean GC half-light radius, \bar{m}_{GC} is the mean GC mass, v_{rms} is the root-mean-square velocity of the GC system (i.e., $\sqrt{3}$ times the line-of-sight velocity dispersion), $R_{\text{GC,max}}$ is the maximum projected galactocentric distance in the galaxy and n_{GC} is the GC number density inside this volume.

Equation 8 has been adapted from Equation A9 in [Leigh & Sills \(2011\)](#).¹ In particular, it has been adapted from a roughly constant-density cluster core² such that for the size

¹ We set f_b and f_t both equal to zero as these are the binary and triple fractions, respectively, in a star cluster. Hence, in the original equation, these terms correct for the fraction of the total number of stars that are isolated

or volume of the region of interest, we adopt the maximum galactocentric distance observed for all GCs in each galaxy.³ It is then straight-forward to compute a GC number density n_{GC} for each galaxy within this volume, by adopting 7 and 10 GCs for, respectively, NGC 1052-DF4 and NGC 1052-DF2 for the total number of GCs inside this volume. For the velocity dispersions of the GC populations within these volumes, we take the likelihood values of 3.2 km s^{-1} and 3.8 km s^{-1} for, respectively, NGC 1052-DF2 ([Van Dokkum et al. 2018b](#)) and NGC 1052-DF4 ([Van Dokkum et al. 2019](#)). Using the indicated GC masses in Table 2 we calculate an average GC mass for each galaxy, and adopt a typical GC size (i.e., r_{GC}) of 20 pc for all galaxies (motivated by a measured mean GC half-light radius of $6.5 \pm 0.5 \text{ pc}$ in NGC 1052-DF2 by [Van Dokkum et al. \(2018b\)](#)). With these parameters, we compute mean GC-GC interaction times corresponding to direct collisions of 460 Gyr and 730 Gyr for, respectively, NGC 1052-DF2 and NGC 1052-DF4. Over a period of 10 Gyr, this implies collision probabilities of only a few percent.

Importantly, the above simple calculations neglect any evolution of the GC populations - i.e., it assumes that what we see now for the GC populations is what has always been there. If the number density of GCs had been higher by a factor of 10 in the past (see e.g. [Fragione & Kocsis 2018](#); [Fragione et al. 2018](#)), then the interaction rates would increase by a factor of 100. This would result in a number of direct GC-GC collisions within a 10 Gyr period, while also ejecting even more GCs from their host galaxy due to strong interactions. This would have contributed to modifying the observed distribution of GC masses and galactocentric radii.

To better quantify the above, we set the GC-GC collision times equal to 1, 2 and 3 Gyr, motivated by the shortest DF timescales found in Section 2.4. We then solve for both the critical number density and the critical number of GCs within the above volumes required for a single GC-GC collision to occur within these times. The result is shown in Figure 4. The upper panel of Figure 4 shows that of order ~ 100 GCs are needed in this volume to have a single GC-GC collision within 1 Gyr (see the solid black and red lines). This implies that, assuming mean GC masses of $2.5 \times 10^5 M_\odot$ and $1.3 \times 10^5 M_\odot$ for, respectively, NGC 1052-DF2 and NGC 1052-DF4, 10 and 7 GC-GC collisions (i.e., corresponding to the observed number of bright GCs in each galaxy) would happen within 10 Gyr and 7 Gyr, respectively.

Given such high collision rates, we would also expect many more GC-GC interactions without collisions (i.e., at larger impact parameters). Driven by the tendency toward energy equipartition, this would contribute to preferentially ejecting the lowest mass GCs from their host galaxies and robbing the more massive GCs of orbital energy and angular momentum, causing them to sink deeper in their host galaxy potentials. This could help to account for the observed unusually high masses and small galactocentric radii, relative to the MW GC population (see Figure 1). A similar result was also recently found by [Madau et al. \(2019\)](#), who considered galaxy-galaxy

singles. For the present problem, we assume that all GCs (the equivalent of stars here in the original equation) are isolated single objects.

² The assumption of a constant density inner core is reasonable over the small spatial extent of the host galaxy that we consider here, since the innermost density profile is not cuspy ([Van Dokkum et al. 2018b, 2019](#)). A more detailed correction accounting for the shape of the inner host galaxy potential would affect the calculated timescales by at most a factor of order unity.

³ We set r_c in Equation A9 to 7.55 kpc in NGC 1052-DF2 and 7.01 kpc in NGC 1052-DF4; see Table 2).

collisions, and suggested that the resulting GCs should be more centrally concentrated due to dissipative effects during the interactions.

Ignoring dissipative effects, the dynamical evolution of the GC mass function should be *statistically deterministic*. Said another way, the fates of individual particles are sensitive to the precise initial conditions, but the evolution of the overall distribution functions are not. To see that this should indeed be the case, consider the following equation:

$$\frac{\partial f_m}{\partial t} + \frac{\partial f_m}{\partial m} \frac{\partial m}{\partial t} = - \frac{\partial}{\partial m} (f_m < \Delta m >) + \frac{1}{2} \frac{\partial^2}{\partial m^2} (f_m < \Delta m^2 >), \quad (9)$$

where $f_m(m)$ is the GC mass function, which is a continuous differentiable function over the range of GC masses of interest (i.e., from the assumed initial minimum GC mass to the initial maximum GC mass), and $< \Delta m >$ and $< \Delta m^2 >$ are first- and second-order diffusion coefficients. The diffusion coefficients can be calculated accordingly:

$$< \Delta m > = \int \Gamma(m) f_m(m) \Delta m d\Delta m \quad (10)$$

and

$$< \Delta m^2 > = \int \Gamma(m) f_m(m) \Delta m^2 d\Delta m, \quad (11)$$

and $\Gamma(m)$ is the mass-dependent collision rate:

$$\Gamma(m) = n(m) \sigma_{\text{coll}}(m) v_{\text{rms}}(m). \quad (12)$$

In the above equation, $n(m)$ and $v_{\text{rms}}(m)$ are the number density and root-mean-square velocities for GCs with mass m , respectively. The collisional cross-section is denoted by $\sigma_{\text{coll}}(m)$, and gives the gravitationally-focused cross-section for collisions involving species of mass m (the total rate for a given mass species can be obtained by integrating the collision rate over the GC mass function). Both the GC number density and root-mean-square velocity are mass-independent initially (Lynden-Bell 1967), and evolve toward a state of energy equipartition at a rate that can be determined using a multi-mass Fokker-Planck equation (see below).

Equation 9 is a Boltzmann-type of equation that quantifies the evolution of a GC population in mass function-space due to direct collisions, starting from a well-mixed (in energy-space, and hence position- and velocity-space) population of GCs as occurs post-violent relaxation. Hence, an episode of violent relaxation provides a well-defined "initial" state (see Lynden-Bell (1967) for more details) from which the subsequent dynamical evolution follows in a *statistically deterministic or causal manner*. Equation 9 assumes conservation of mass, energy and angular momentum, so does not account for stellar or binary evolution. It can, in principle, be combined with a multi-mass Fokker-Planck model to simultaneously quantify the dynamical evolution of the GC mass function in position- and velocity-space.

To summarize, the GC mass function will evolve due to two separate effects: direct collisions quantified by the Boltzmann-type equation in mass-space (i.e., Equation 9), and evaporation induced by two-body relaxation quantified via a multi-mass Fokker-Planck 'master equation'. These two mechanisms preferentially impact, respectively, the high- and low-mass ends of the GC mass function. The dynamical evolution of the low-mass end of the mass function is thus the only mass loss from the cluster. This can be quantified in time and space via a multi-mass Fokker-Planck equation, and the mass function evolved accordingly. As with the high-mass end, the subsequent evolution of the low-mass end of the mass

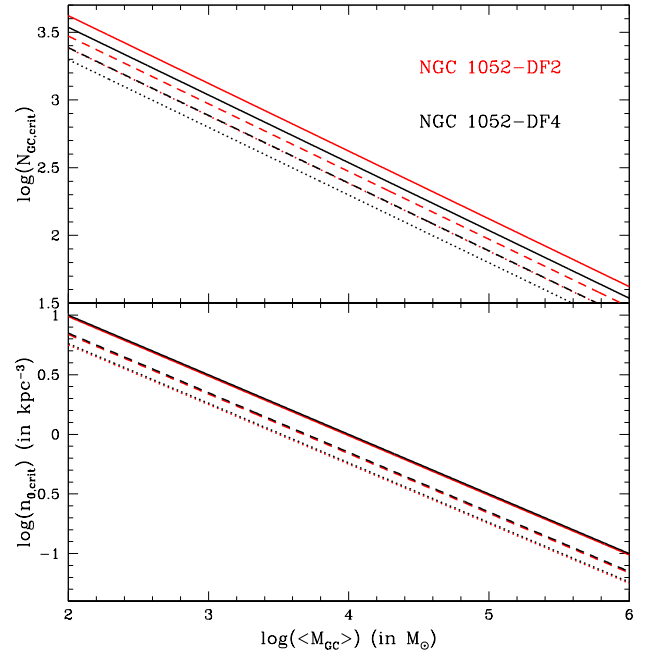


Figure 4. The critical number density (bottom panel) and critical number (top panel) of GCs within the specified volumes (see text) required for a single GC-GC collision to occur within 1, 2 and 3 Gyr. The solid, dashed and dotted lines correspond to, respectively, 1, 2 and 3 Gyr. As before, NGC 1052-DF4 and NGC 1052-DF2 are indicated by, respectively, the black and red lines.

function is statistically deterministic and can be easily parameterized (see Webb & Leigh (2015) for more details).

2.6. Quantifying the dynamical evolution of a GC population using Collision Rate Diagrams

In Figure 5 we show the time evolution of the number fractions of three different GC species. Each species has a unique combination of mass and radius. We adopt GC types A, B and C and (conservatively) assume that they adhere to a ratio in mass and size of $1:2:\geq 3$, respectively (the units are not relevant for the *relative* rates, only the *absolute* rates).⁴ We then follow the procedure described in Leigh et al. (2017) and expanded upon in Leigh et al. (2018) to calculate the relative collision rates for different particle types. We plot the fractions of B- and C-type particles on the x- and y-axes, respectively, and assume $1 = f_A + f_B + f_C$. The different segmented regions indicate the parameter space where different collision scenarios each dominate.

As an initial illustrative example, we focus on larger impact parameter interactions than correspond to direct collisions, to quantify the preferential ejection of lower mass GCs. For simplicity, we assume that interactions between different particle types always eject the lowest-mass GC from the galaxy. Interactions between identical particles are assumed to result in the ejection of one of the two particles. These assumptions are over-simplified but capture the general trends expected from simple conservation of linear momentum and energy, given the (mass-independent) initial conditions expected post-violent relaxation (due to, for example, a recent galaxy-galaxy collision (Lynden-Bell 1967; Madau et al. 2019)). We sample

⁴ Steeper mass ratios would only accelerate the basic trends we report here, rapidly driving host galaxies to very high fractions of only the most massive of their original GCs. Hence, our assumption here is the most conservative possible, in this regard.

the allowed parameter space of initial conditions uniformly in the f_B - f_C -plane, and follow the subsequent time evolution in the f_B - f_C -plane until only one type of GC remains.

As is clear from the dotted red lines in Figure 5, the evolution is always toward very high fractions of C-type particles, which correspond to the most massive GCs given our assumptions. Within the context of our hypothesis, this is roughly consistent with what is currently observed in NGC 1052-DF2 and NGC 1052-DF4, if the observed GCs represent the remains of once much richer GC populations. *Figure 5 suggests that the present-day observed relative number fractions can be used to uniquely constrain the initial number fractions, since every trajectory (depicted by the red lines) is unique and does not cross any other lines (excluding evolution along the outer boundaries).*

Another illustrative example is shown in Figure 5, by the solid red lines. Here, we focus on smaller impact parameters, leading to direct collisions. That is, if a close interaction occurs, then so must a direct collision if at the distance of closest approach the stars are closer than the sum of their radii. We adopt the mass ratios $1:2:\geq 3$ corresponding to A:B:C, such that collisions tend to quickly over-populate the C-type particles. As is clear from this simple exercise, the flow lines in the f_B - f_C -plane are maximally directed toward $f_C \sim 1.0$ on short timescales.

Finally, we apply Figure 5 to the GC populations in both NGC 1052-DF2 and NGC 1052-DF4. To compute the fractions of particle types, we define A-, B- and C-type particles to correspond to the mass intervals, respectively, $1 - 4 \times 10^5 M_\odot$, $4 - 8 \times 10^5 M_\odot$ and $8 - 12 \times 10^5 M_\odot$. According to Table 2, this gives $f_A = 0.2$, $f_B = 0.6$ and $f_C = 0.2$ for NGC 1052-DF2 (red cross) and $f_A = 0.3$, $f_B = 0.6$ and $f_C = 0.1$ for NGC 1052-DF4 (black cross).

The key point to take away from these simple examples is that, given a hypothesized dynamical evolution for a GC population post-galaxy-galaxy interaction, there is a strong connection between the adopted initial conditions and the present-day observed state of the system. *More specifically, from these simple examples, we see that knowing the observed present-day relative GC number fractions and positing a concrete hypothesis for the subsequent dynamical evolution via collisions and/or ejections, we are able to use the present-day observed number fractions to uniquely constrain the initial relative number fractions prior to any internal dynamical processing.* Thus, the method will allow for a comparison between the candidate galaxy's *past or pre-dynamically processed* GC luminosity function (and GC specific frequency, etc.) and those of other galaxies. Given a sensible assumption for the primordial GC luminosity function (see Fragione et al. (2018) for more details) in the progenitor galaxy, if a strong galaxy-galaxy interaction did occur then one can compute the precise effects of the interaction on the host's GC population (i.e., which GCs collided and which were ejected and/or stripped?).

This motivates the need to perform additional simulations of strong galaxy-galaxy interactions and their implications for pre-existing GC populations, to help populate Figure 5 and better understand the dependence on the initial conditions and the effects of strong interactions. Our results predict a paucity of low-mass GCs relative to a scenario without any prior host galaxy-galaxy interaction, triggering an episode of violent relaxation and the subsequent internal dynamical evolution of the host galaxy's GC population. This motivates a deeper and more thorough observational campaign to try to identify

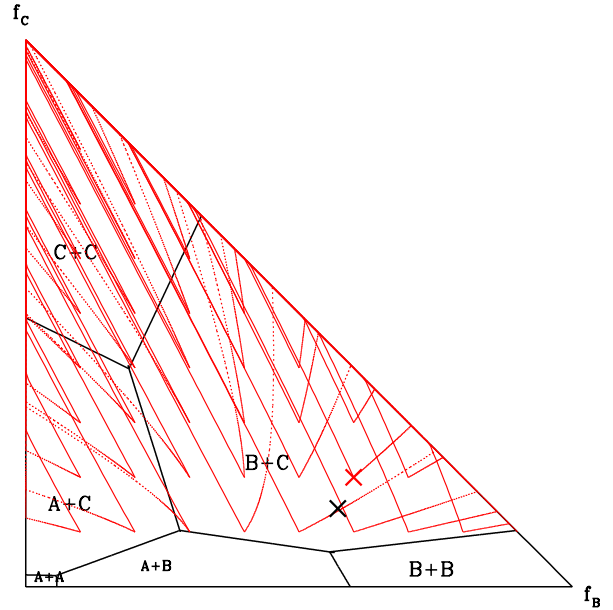


Figure 5. Collision Rate Diagram (Leigh et al. 2017, 2018) for GC populations in the NGC 1052 group. We consider three different GC species for a given galaxy, each with its own assumed mass and size, and show the time evolution of their relative number fractions. We adopt GC types A, B and C and assume that they adhere to a ratio in mass and size of $1:2:\geq 3$, respectively (the units are not relevant for the relative rates, only the absolute rates; see text for more details). Following the procedure described in the text, we plot the fractions of B- and C-type particles on the x- and y-axes respectively, and assume that $1 = f_A + f_B + f_C$. The different segmented regions indicate where different collision scenarios each dominate. The solid red lines show the time evolution in the f_B - f_C -plane for each assumed set of initial relative number fractions. Finally, the red and black crosses show the observed fractions for, respectively, NGC 1052-DF2 and NGC 1052-DF4 (see text for details).

GCs associated with NGC 1052-DF2 and NGC 1052-DF4, to probe further down the GC luminosity function (similar to what was done in Trujillo et al. (2019)). This would allow us to improve our analysis in Figure 5, and populate it with more robust empirical data. In turn, this would facilitate more stringent constraints on the conditions post-interaction and, specifically, the initial GC mass function.

3. DISCUSSION

In this paper, we consider the origins of the recently discovered ultra-diffuse DM-free galaxies NGC 1052-DF2 and NGC 1052-DF4. This is because we are presenting a new method for uniquely constraining the past dynamical evolution of GC populations thought to have undergone a prior episode of violent relaxation. The presently observed properties and numbers of the remaining GCs is all that is required to apply the method robustly. We consider two different scenarios to account for the observed GC properties, both involving a prior strong interaction with a more massive galaxy that stripped the host galaxies of their DM. These are: (1) The progenitors of NGC 1052-DF2 and NGC 1052-DF4 either had no massive GCs prior to the interaction, such that the interaction triggered the formation of the observed massive GCs (e.g. Silk 2019); or (2) the progenitors had a substantial GC population, and the interaction triggered an episode of violent relaxation in the host galaxy GC population. In the latter case, violent relaxation would significantly perturb the GC orbits, mixing them thoroughly in phase-space. This

should push some GCs to become highly eccentric, while also ejecting loosely bound GCs. These ejected GCs would either become "free-floating", or end up gravitationally bound to the more massive interloping galaxy.

As described in Section 1, a close interaction between two galaxies with a large mass ratio between them could strip them of their DM content by ejecting the stars and gas in the progenitor's disk. This is also the case in the event of a direct high-velocity collision (e.g. [Silk 2019](#)). During a close interaction, it has been shown (e.g. [Nusser 2019](#)) that, when the DM halo is ejected, the left-over stars and gas comprising the galaxy more or less retain the velocity dispersion of their much more massive progenitor. Similarly, a direct collision will deposit kinetic energy, only some of which is dissipated by the gas. Thus, immediately after a close interaction or even collision, DM-stripped galaxies should be highly super-virial, and will expand by the virial theorem. Re-virialization should occur on a crossing time, which for NGC 1052-DF4 happens to currently be ~ 0.2 Gyr within the half-light radius, assuming a half-light radius of 1.6 kpc and a stellar velocity dispersion of 7 km s^{-1} ([Van Dokkum et al. 2019](#)) (and NGC 1052-DF2 therefore has a similar crossing time, given the similar properties of these two galaxies). If the progenitor galaxies were initially more compact than is currently observed, then this would only reduce the crossing time, which is already comparable to the shortest DF timescale for our sample of GCs, at least in NGC 1052-DF4. It therefore seems likely that any such stripping event, whether it be a strong close interaction or a direct high-velocity collision, would produce a remnant galaxy that should expand. *This could contribute to, and perhaps even entirely account for, their observed ultra-diffuse state* (e.g. [Silk 2019](#)).

Is it plausible that both NGC 1052-DF2 and NGC 1052-DF4 experienced a recent close interaction with another galaxy in the NGC 1052 group?⁵ [Van Dokkum et al. \(2018a\)](#) showed that NGC 1052-DF2 could certainly have recently experienced a close interaction with the most massive galaxy in the group, namely NGC 1052, given their very close proximity in projection. NGC 1052-DF4 lies roughly a factor of two further from NGC 1052 in projection, relative to NGC 1052-DF2. Hence, it is also entirely plausible that it too experienced a close interaction with NGC 1052 in the recent past. For NGC 1052-DF4, however, another galaxy lies even closer to it in projection. This is NGC 1035, which lies at a projected distance of 23 kpc from NGC 1052-DF4 and has a relative velocity of 204 km s^{-1} . Assuming a relative velocity at infinity of 110 km s^{-1} ([Cohen et al. 2018](#)), which is equal to the observed line-of-sight velocity dispersion in the NGC 1052 group, and the minimum possible 3D distance of 23 kpc, we compute an interaction time of only ~ 0.02 Gyr, which is roughly an order of magnitude less than our inferred upper limit from the GC DF timescales (see Figure 3) for the time since a close interaction between NGC 1052-DF4 and another galaxy in the NGC 1052 group must have occurred. Hence it is entirely feasible, but by no means guaranteed, that NGC 1052-DF4 very recently had a close interaction with NGC 1035. We conclude that the proposed scenario for stripping both NGC 1052-DF2 and NGC 1052-DF4 of their DM, namely a recent close interaction with a nearby more massive galaxy, is plausible.

3.1. Implications from different interaction scenarios

⁵ Here we note that a direct high-velocity collision would not leave behind an interloping galaxy in the group to search for.

In this section, we consider how the observed properties of NGC 1052-DF2 and NGC 1052-DF4, as well as of their observed GC populations, should change for different interaction scenarios, given our hypothesis of a strong galaxy-galaxy interaction having occurred some time in the past. We consider two different scenarios: (1) The progenitors of NGC 1052-DF2 and NGC 1052-DF4 either had no massive GCs prior to the interaction, and the interaction triggered the formation of the observed massive GCs; or (2) the progenitors had substantial GC populations initially, which were significantly perturbed during the interaction, undergoing an episode of violent relaxation ([Lynden-Bell 1967](#)).

3.1.1. Scenario 1: Did the galaxy-galaxy interaction cause the formation of the observed massive GCs?

In this scenario, we assume that the progenitors of NGC 1052-DF2 and NGC 1052-DF4 recently experienced a strong galaxy-galaxy interaction, and that these hosts initially contained significant mass in gas rotating with their stars. In this scenario, the more massive galaxy ejects the stars and gas from the DM halo, if the gas is pulled along with the stars, which occurs for comparable orbits (i.e., the spin and orbital frequencies are well-matched, maximizing the magnitude of the effect) and the correct prograde orientation of the interaction. If the gas were to collect at the bottom of the potential well of the remnant galaxy, the gas densities could become sufficiently high to trigger GC formation in an extreme high-pressure environment, forming more massive GCs at a given cloud density (e.g. [Murray 2009](#); [Silk 2019](#)). A similar scenario was mostly recently considered by [Silk \(2019\)](#) who proposed high-velocity fast collisions, which could have produced simultaneous triggering of over-pressurized dense clouds that form preferentially massive globular clusters.

This scenario immediately predicts stellar ages for the constituents of the GCs observed in NGC 1052-DF2 and NGC 1052-DF4, that are commensurate with the time since the strong interaction occurred. Hence, naively, this could predict younger (and hence bluer) GCs relative to stars in the field of their host galaxy (and also relative to the GCs described in the below scenario). Said another way, the minimum DF timescale of all ten/seven GCs in NGC 1052-DF2/NGC 1052-DF4 can be used to put a constraint on the minimum time ago the interactions must have occurred. For NGC 1052-DF2 and NGC 1052-DF4, these minimum times would be, respectively, ~ 7 Gyr and ~ 1 Gyr.⁶

We close this section with a brief review of its predictions:

- The observed massive GCs should be younger than the stars comprising their host galaxy. Their integrated colours should thus be bluer than that of the host. If some GCs are retained from the progenitor galaxy, then the GC colour distribution should appear bi-modal.
- The observed GC luminosity function should be top-heavy and centrally concentrated (expected for GC formation in high-pressure gas-rich environments), with a significant paucity of low-mass GCs.
- If indeed some GCs have present-day DF timescales that are much shorter than a Hubble time, the shortest of these can be used to constrain the time since the hypothetical galaxy-galaxy interaction or collision occurred,

⁶ But, again, these exact numbers should be taken with a grain of salt, as described previously in the text.

which is needed to rid the host of its DM. In the case of a very strong close interaction with another perturbing galaxy, this can be converted in to a volume centred on each galaxy within which the more massive perturbing galaxy should reside.

3.1.2. Scenario 2: Did the galaxy-galaxy interactions significantly perturb pre-existing GC orbits?

The expected response of a system of GCs to an episode of violent relaxation is highly collisional, as the system tries to recover a Maxwellian distribution of velocities. That is, the subsequent dynamical evolution is governed by the physics of collisional dynamics, which deterministically connects the initial conditions of the GC populations (i.e., immediately post-violent relaxation) to their final currently observed states.

If the progenitors of NGC 1052-DF2 and NGC 1052-DF4 both had substantial GC populations before the interaction, the tidal force from the massive perturber would not only perturb them on to highly modified likely eccentric orbits, but also unbind the most tenuously bound GCs. The subsequent collisional evolution back toward energy equipartition and a Maxwellian distribution of orbital velocities will also eject preferentially low-mass GCs, removing further energy and angular momentum from the most massive GCs and helping to deliver them deeper into the host galaxy potential. This could predict free-floating GCs somewhere close to NGC 1052-DF2 and NGC 1052-DF4 on the plane of the sky that are not bound to any galaxy. The interloping massive galaxy (e.g., NGC 1052) could also accrete GCs from the perturbed galaxies, which could be identified if significant age, chemical, etc. differences happen to exist between the native and accreted GCs. However, if the interaction happened sufficiently far in the past, any free-floating GCs would have had sufficient travel time to have become difficult, if not impossible, to identify observationally.

Is it possible that the observed GCs in both NGC 1052-DF2 and NGC 1052-DF4 began much further out in their host galaxy potential, and have simply been caught in the act of spiraling inward due to DF? This was recently proposed by Dutta Chowdhury, van den Bosch & van Dokkum (2019), who use a suite of 50 multi-GC N-body models to follow the orbital decay of the GCs. They find that over ~ 10 Gyr many GCs experience significant orbital decay due to DF, whereas others evolve much less. In their simulations, they find that a combination of reduced DF in the galaxy core and GC-GC scattering keeps the GCs buoyant in their host galaxy potential, such that they have not yet sunk to its centre. The authors conclude that if NGC 1052-DF2 is indeed devoid of DM, then at least some of its GCs must have formed further out before spiraling in to their current locations, and that the GC system was likely more extended in the past. Nusser (2018) used a similar approach to study DF in NGC 1052-DF2 using N-body simulations, and found much the same thing, but with the added correction that in some simulation realizations GCs do decay all the way to the centre of their host galaxy. Both of the conclusions arrived at in these papers via more detailed N-body simulations are consistent with the overall results reported in this paper.

If Van Dokkum et al. (2019) indeed caught one out of seven GCs in NGC 1052-DF4 at the end of its spiral-in phase (see Figure 3), then why have no other GCs already spiraled in to the nucleus? Provided the true DF timescales for these three GCs are close to our calculations, the lack of a central NSC is indeed puzzling. If other DM-free galaxies are identified in

the NGC 1052 group (or any other), the probability that they will host a central NSC could be high, produced by DF of GCs formed or perturbed onto orbits deeper in the host galaxy potential during the close galaxy-galaxy interaction presumed to have stripped its host of its DM.

Indeed, the observational results of Graham & Spitler (2009), comparing super-massive black hole (SMBH) and NSC masses as a function of their host galaxy mass, suggest that both NGC 1052-DF2 and NGC 1052-DF4 are of sufficiently low mass that their central regions should be dominated by an NSC (if a central massive object, either NSC or SMBH, is present at all), rather than an SMBH. And yet, close inspection of Figure 1 in Van Dokkum et al. (2019) suggests that no central nuclear star cluster (NSC) is present in either NGC 1052-DF2 or NGC 1052-DF4. Alternatively, the lack of a central NSC could be pointing toward a stalling of DF as GCs reach the centre of their host galaxy, either due to GC-GC interactions, the inclusion of a radial-dependence to the Coulomb logarithm, etc. (see Dutta Chowdhury, van den Bosch & van Dokkum (2019) for more details).

We close this section with a brief review of its predictions:

- Relative to galaxies where GC-GC collisions are not expected to happen, this predicts a top-heavy GC mass function, with the brightest and hence most massive GCs residing at small galactocentric distances. This last effect should be enhanced via the fact that direct GC-GC collisions dissipate both orbital energy and angular momentum, causing the collision products to fall even deeper in to the host galaxy potential.
- The observed GCs should have roughly the same age as the stars comprising their host galaxy. Their integrated colours, corresponding to old stellar populations, should thus be very similar to that of their host.
- The distribution of (3D) GC velocities should be close to isotropic.
- The most tenuously bound GCs in the galaxy progenitors could have been stripped or accreted on to the more massive interloping galaxy (e.g., NGC 1052). This could predict non-native GCs in the (hypothetical) more massive perturbing galaxy that were accreted during the interaction. Alternatively, it could predict free-floating GCs lingering as debris in the vicinity of each galaxy post-interaction. The observability of such free-floating GCs is, however, likely to be very sensitive to exactly *when* the hypothetical galaxy-galaxy interaction occurred. If our computed DF timescales are accurate, identifying these free-floating galaxies should be most probable for NGC 1052-DF4, given its much shorter constraint on the time since the interaction occurred. That is, any free-floating GCs produced would only have a travel time of ~ 1 Gyr.

4. SUMMARY

In this paper, we present a new method for uniquely constraining the past dynamical evolution of GC populations thought to have undergone a past episode of violent relaxation. The presently observed properties and numbers of the remaining GCs are all that is required to apply the method robustly. We consider two different scenarios to account for the

observed GC properties, both involving a prior strong interaction with a more massive galaxy. The encounter is hypothesized to have both stripped NGC 1052-DF2/NGC 1052-DF4 of their DM halos and either triggered their formation or an episode of violent relaxation in the progenitor GC population.

We first consider the currently observed state of the GC populations in NGC 1052-DF2 and NGC 1052-DF4, from which we infer and quantify the implications for their past and future states. We calculate the DF timescales for infall to the central nucleus for the GCs in both galaxies. We find that two out of ten GCs in NGC 1052-DF2 and one out of seven in NGC 1052-DF4 have DF timescales less than a Hubble time. In principle, the shortest DF time should put a limit on the time since any past galaxy-galaxy interaction occurred.

For each galaxy, we go on to calculate the critical number of GCs and the critical GC number density needed for a given number of direct GC-GC interactions/collisions to have occurred since the hypothesized galaxy-galaxy interaction. This is done by setting the number of collisions equal to the observed numbers of bright GCs in each galaxy, and requiring that the evolution occur on a timescale shorter than the minimum DF time in each galaxy. The results of this analysis show that significant collisional evolution of a richer GC population than is currently observed could have feasibly evolved dynamically to produce the currently observed distributions of GC masses and galactocentric radii. This would contribute both to the observed top-heavy GC mass functions and their centrally concentrated galactocentric distances, and motivates more detailed N-body simulations in future work.

We further present a novel method to constrain the initial GC mass functions prior to the (hypothesized) chaotic dynamical evolution that should occur post-galaxy-galaxy interaction. To this end, we apply a Collision Rate Diagram to re-wind the clock and constrain the relative numbers of GCs in different mass bins at the time of interaction. This simple exercise motivates obtaining more complete observations of the GC luminosity functions in these galaxies, which can then be used to constrain the origins of the hypothesized DM-free galaxies, by combining the method presented here with a suite of numerical simulations.

ACKNOWLEDGMENTS

We thank Adi Nusser, Asher Wassermann and Pieter van Dokkum for their insightful comments on an early version of the paper. We are grateful to Asher Wasserman for providing data of the star clusters, and Doug Geisler for useful discussions. NWCL is gratefully supported by a Fondecyt Iniciación grant (11180005). GF is supported by the Foreign Postdoctoral Fellowship Program of the Israel Academy of Sciences

and Humanities. GF also acknowledges support from an Arskin postdoctoral fellowship.

REFERENCES

- Abraham R. G., van Dokkum P. G. 2014, *PASP*, 126, 55
 Arca-Sedda M., Capuzzo-Dolcetta R. 2017, *MNRAS*, 464, 3060
 Behroozi P. S., Wechsler R. H., Conroy C. 2013, *ApJ*, 770, 57
 Binney J., Tremaine S., 1987, *Galactic Dynamics* (Princeton: Princeton University Press)
 Chandrasekhar S. 1943, *ApJ*, 596, 34
 Choksi N., Gnedin O. Y. 2018, (arXiv:1810.01888)
 Dutta Chowdhury D., van den Bosch F. C., van Dokkum P. 2019, submitted (arXiv:1902.05959)
 Cohen Y., van Dokkum P., Danieli S., Romanowsky A. J., Abraham R., Merritt A., Zhang J., Mowla L., et al. 2018, *ApJ*, 868, 96
 Colpi M., Mayer L., Governato F. 1999, *ApJ*, 545, 720
 D’Onghia E., Besla G., Cox T. J., Hernquist L. 2009, *Nature*, 460, 605
 Dutta Chowdhury D., van den Bosch F. C., van Dokkum P. 2019, arXiv:1902.05959
 Emsellem E. et al. 2019 *A&A*, 625, A76
 Fensch J. et al. 2019, *A&A*, 625, A77
 Forbes D. A., Read, J. I., Gieles, M., Collins, M. L. M. 2018, *MNRAS*, 481, 5592
 Fragione G., Kocsis B. 2018, *Phys. Rev. Lett.*, 121, 161103
 Fragione G., Leigh N., Ginsburg I., Kocsis B. 2018, *ApJ*, 867, 119
 Gnedin O. Y., Hernquist L., Ostriker J. P. 1999, *ApJ*, 514, 109
 Gnedin O. Y., Ostriker J. P., Tremaine S. 2014, *ApJ*, 785, 71
 Graham A. W., Spitler L. R., *MNRAS*, 397, 2148
 Harris W. E. 1996, *AJ*, 112, 1487 (2010 update)
 Harris W. E., Gretchen L. H., Alessi M. 2013, *ApJ*, 772, 82
 Harris W. E. 2016, *ApJ*, 151, 102
 Kroupa P., et al. 2019, *Nature*, 561, E4
 Lacey C., Cole S. 1993, *MNRAS*, 262, 627
 Laporte C. F. P., Agnello A., Navarro J. F. 2019, *MNRAS*, 484, 245
 Leigh N., Sills A. 2011, *MNRAS*, 410, 2370
 Leigh N. W. C., Geller A. M., Shara M. M., Garland J., Clees-Baron H., Ahmed A. 2017, *MNRAS*, 471, 1830
 Leigh N. W. C., Geller A. M., Shara M. M., Baugher L., Hierro V., Ferreira De’ A., Teperino E. 2018, *MNRAS*, 480, 3062
 Lynden-Bell D. 1967, *MNRAS*, 136, 101
 Mac Low M. M., Ferrara A. 1999, *ApJ*, 513, 142
 Madau P., Lupi A., Diemand J., Burkert A., Lin D. N. C. 2019, *ApJ*, submitted (arXiv:1905.08951)
 Mayer L., Kazantzidis S., Mastropietro C., Wadsley J. 2007, *Nature*, 445, 738
 Murray N. 2009, *ApJ*, 691, 946
 Nusser A. 2018, *ApJL*, 863, L17
 Nusser A. 2019, *MNRAS*, 484, 510
 Taylor M. A., Puzia T. H., Gomez M., Woodley K. A. 2015, *AJ*, 805, 65
 Terzic B., Graham A. W. 2005, *MNRAS*, 362, 197
 Tremaine S. D., Ostriker J. P., Spitzer L. Jr. 1975, *ApJ*, 196, 407
 Trujillo I., Beasley M. A., Borlaff A., Carrasco E. R., Di Cintio A., Filho M., Mionelli M., Montes M., et al. 2019, *MNRAS*, 486, 1192
 Silk J. 2019, *MNRAS*, accepted (arXiv:1905.13235)
 van Dokkum P., Danieli S., Cohen Y., Merritt A., Romanowsky A. J., Abraham R., Brodie J., Conroy C., Lokhorst D., Mowla L., O’Sullivan E., Zhang J. 2018a, *Nature*, 555, 629
 van Dokkum P., Cohen Y., Danieli S., Kruijssen J. M., Romanowsky A. J., Merritt A., Abraham R., Brodie J., Conroy C., Lokhorst D., Mowla L., O’Sullivan E., Zhang J. 2018b, *ApJ*, 856, 30
 van Dokkum P., Danieli S., Cohen Y., Romanowsky A. J., Conroy C. 2018c, *ApJL*, 864, 18L
 van Dokkum P., Danieli S., Abraham R., Conroy C., Romanowsky A. J. 2019, submitted (arXiv:1901.05973)
 Webb, J.J., Leigh N. W. C. 2015, *MNRAS*, 453, 3278